

Upper limits to the SN1006 multi-TeV gamma-ray flux from H.E.S.S. observations

F. Aharonian¹, A.G. Akhperjanian², K.-M. Aye³, A.R. Bazer-Bachi⁴, M. Beilicke⁵, W. Benbow¹, D. Berge¹, P. Berghaus⁶*, K. Bernlöhr^{1,7}, C. Boisson⁸, O. Bolz¹, C. Borgmeier⁷, F. Breitling⁷, A.M. Brown³, J. Bussons Gordo⁹, P.M. Chadwick³, L.-M. Chounet¹⁰, R. Cornils⁵, L. Costamante^{1,20}, B. Degrange¹⁰, A. Djannati-Atai⁶, L.O'C. Drury¹¹, G. Dubus¹⁰, T. Ergin⁷, P. Espigat⁶, F. Feinstein⁹, P. Fleury¹⁰, G. Fontaine¹⁰, S. Funk¹, Y.A. Gallant⁹, B. Giebels¹⁰, S. Gillessen¹, P. Goret¹², C. Hadjichristidis³, M. Hauser¹³, G. Heinzelmann⁵, G. Henri¹⁴, G. Hermann¹, J.A. Hinton¹, W. Hofmann¹, M. Holleran¹⁵, D. Horns¹, O.C. de Jager¹⁵, I. Jung^{1,13}**, B. Khélifi¹, Nu. Komin⁷, A. Konopelko^{1,7}, I.J. Latham³, R. Le Gallou³, A. Lemièr⁶, M. Lemoine¹⁰, N. Leroy¹⁰, T. Lohse⁷, A. Marcowith⁴, C. Masterson^{1,20}, T.J.L. McComb³, M. de Naurois¹⁶, S.J. Nolan³, A. Noutsos³, K.J. Orford³, J.L. Osborne³, M. Ouchrif^{16,20}, M. Panter¹, G. Pelletier¹⁴, S. Pita⁶, G. Pühlhofer^{1,13}, M. Punch⁶, B.C. Raubenheimer¹⁵, M. Raue⁵, J. Raux¹⁶, S.M. Rayner³, I. Redondo^{10,20***}, A. Reimer¹⁷, O. Reimer¹⁷, J. Ripken⁵, L. Rob¹⁸, L. Rolland¹⁶, G.P. Rowell¹, V. Sahakian², L. Sauge¹⁴, S. Schlenker⁷, R. Schlickeiser¹⁷, C. Schuster¹⁷, U. Schwanke⁷, M. Siewert¹⁷, H. Sol⁸, R. Steenkamp¹⁹, C. Stegmann⁷, J.-P. Tavernet¹⁶, C.G. Théoret⁶, M. Tluczykont^{10,20}, D.J. van der Walt¹⁵, G. Vasileiadis⁹, P. Vincent¹⁶, B. Visser¹⁵, H.J. Völk¹, and S.J. Wagner¹³

¹ Max-Planck-Institut für Kernphysik, P.O. Box 103980, D 69029 Heidelberg, Germany

² Yerevan Physics Institute, 2 Alikhanian Brothers St., 375036 Yerevan, Armenia

³ University of Durham, Department of Physics, South Road, Durham DH1 3LE, U.K.

⁴ Centre d'Etude Spatiale des Rayonnements, CNRS/UPS, 9 av. du Colonel Roche, BP 4346, F-31029 Toulouse Cedex 4, France

⁵ Universität Hamburg, Institut für Experimentalphysik, Luruper Chaussee 149, D 22761 Hamburg, Germany

⁶ Physique Corpusculaire et Cosmologie, IN2P3/CNRS, Collège de France, 11 Place Marcelin Berthelot, F-75231 Paris Cedex 05, France

⁷ Institut für Physik, Humboldt-Universität zu Berlin, Newtonstr. 15, D 12489 Berlin, Germany

⁸ LUTH, UMR 8102 du CNRS, Observatoire de Paris, Section de Meudon, F-92195 Meudon Cedex, France

⁹ Groupe d'Astroparticules de Montpellier, IN2P3/CNRS, Université Montpellier II, CC85, Place Eugène Bataillon, F-34095 Montpellier Cedex 5, France

¹⁰ Laboratoire Leprince-Ringuet, IN2P3/CNRS, Ecole Polytechnique, F-91128 Palaiseau, France

¹¹ Dublin Institute for Advanced Studies, 5 Merrion Square, Dublin 2, Ireland

¹² Service d'Astrophysique, DAPNIA/DSM/CEA, CE Saclay, F-91191 Gif-sur-Yvette, France

¹³ Landessternwarte, Königstuhl, D 69117 Heidelberg, Germany

¹⁴ Laboratoire d'Astrophysique de Grenoble, INSU/CNRS, Université Joseph Fourier, BP 53, F-38041 Grenoble Cedex 9, France

¹⁵ Unit for Space Physics, North-West University, Potchefstroom 2520, South Africa

¹⁶ Laboratoire de Physique Nucléaire et de Hautes Energies, IN2P3/CNRS, Universités Paris VI & VII, 4 Place Jussieu, F-75231 Paris Cedex 05, France

¹⁷ Institut für Theoretische Physik, Lehrstuhl IV: Weltraum und Astrophysik, Ruhr-Universität Bochum, D 44780 Bochum, Germany

¹⁸ Institute of Particle and Nuclear Physics, Charles University, V Holesovickach 2, 180 00 Prague 8, Czech Republic

¹⁹ University of Namibia, Private Bag 13301, Windhoek, Namibia

²⁰ European Associated Laboratory for Gamma-Ray Astronomy, jointly supported by CNRS and MPG

Received / Accepted

Abstract. Observations of the shell-type supernova remnant SN1006 have been carried out with the H.E.S.S. system of Cherenkov telescopes during 2003 (18.2h with two operating telescopes) and 2004 (6.3h with all four telescopes). No evidence for TeV γ -ray emission from any compact or extended region associated with the remnant is seen and resulting upper limits at the 99.9% confidence level are up to a factor 10 lower than previously-published fluxes from CANGAROO. For SN1006 at its current epoch of evolution we give limits for a number of important global parameters. Upper limits on the γ -ray luminosity (for $E=0.26$ to 10 TeV, distance $d=2$ kpc) of $L_\gamma < 1.7 \times 10^{33}$ erg s⁻¹, and the total energy in corresponding accelerated protons, $W_p < 1.6 \times 10^{50}$ erg (for proton energies $E_p \sim 1.5$ to 60 TeV and assuming the lowest value $n = 0.05$ cm⁻³ of the ambient target density discussed in literature) are estimated. Extending this estimate to cover the range of proton energies observed in the cosmic ray spectrum up to the knee (we take here $E_p \sim 1$ GeV to 3 PeV, assuming a differential particle index -2) gives $W_p < 6.3 \times 10^{50}$ erg. A lower limit on the post-shock magnetic field of $B > 25 \mu\text{G}$ results when considering the synchrotron/inverse-Compton framework for the observed X-ray flux and γ -ray upper limits.

Key words. Gamma rays: observations -

1. Introduction

Observations of shell-type supernova remnants (SNR) at multi-GeV to TeV γ -ray energies have long been motivated by the idea that they are the prime source of hadronic cosmic-ray (CR) acceleration in our galaxy (see for example Drury, Aharonian & Völk 1994 and Naito & Takahara 1994). The detection of non-thermal X-ray emission from the young shell-type SNR SN1006 (Koyama et al. 1995, Allen et al. 2001) suggests that SN1006 is a site of electron acceleration to multi-TeV energies. Subsequent arc-second resolution results from Chandra (Long et al. 2003, Bamba et al. 2003) reveal the presence of several bright non-thermal X-ray arcs concentrating in the NE and SW regions of the SNR, which likely trace the location of strong shocks where at least electrons are accelerated. These, and similar X-ray results from a number of other SNR over the past ten years, have provided a priority list of such targets for ground-based γ -ray telescopes. The results of CANGAROO-I (Tanimori et al. 1998), suggesting TeV γ -ray emission from the NE rim of SN1006 supported the notion that this SNR is capable of electron acceleration up to energies ~ 100 TeV, when interpreted in the synchrotron/inverse-Compton (IC) framework. The TeV photon spectrum is compatible with a power law of photon index $\Gamma \sim 2.3$ (for $dN/dE \sim E^{-\Gamma}$) in the energy range 1.5 to 20 TeV (Naito et al. 1999, Tanimori et al. 2001). Later data from the CANGAROO-II 10 metre telescope also revealed SN1006 as an emitter of TeV γ -rays (Hara et al. 2001), yielding a compatible energy spectrum. The stand-alone HEGRA CT1 telescope has also reported a significant excess in observations taken at very large zenith angles and therefore at a high energy threshold $E > 18$ TeV (Vitale et al. 2003).

The interpretation of these X-ray and ground-based γ -ray results generally involves the electronic synchrotron/IC and/or hadronic π^0 -decay channels. Either channel can dominate, depending on, for example, the density of ambient matter n and magnetic field strength B . Detailed sampling of the γ -ray spectra and morphology are required to disentangle the electronic and hadronic components. The H.E.S.S. (High Energy Stereoscopic System) experiment, the first of the next-generation ground-based γ -ray detectors to utilise the stereoscopic technique, has observed SN1006 during 2003 and 2004. The prime motivation of these observations, apart from confirmation of the CANGAROO results, has been to de-

Table 1. Summary of H.E.S.S. observations of SN1006.

Obs. Period	Runs	ON source livelime [h]	^a $\langle z \rangle$	Telescopes in use
Mar 2003	18	4.1	23.9	2
Apr 2003	21	5.0	25.4	2
May 2003	25	9.1	23.3	2
2003 Total	65	18.2	24.0	
May 2004	15	6.3	28.5	4
All Total	80	24.5	25.0	

a: Average zenith angle [deg] of observations.

termine the nature of any 100 GeV to TeV γ -ray emission from SN1006.

Operating in the Southern Hemisphere, the H.E.S.S. experiment consists of four identical Cherenkov telescopes each with mirror area ~ 107 m² (Bernlöhr et al. 2003, Cornils et al. 2003, Vincent et al. 2003). All four telescopes have been operating since December 2003. Here, we present results using H.E.S.S. data taken during 2003 (two telescopes operating in stereo but with considerable dead time of $\sim 50\%$ due to the lack of a central trigger system 2004). The four-telescope mode of 2004 with the central trigger is the most sensitive configuration for H.E.S.S. We update here previous results of Masterson et al. (2003) which utilised a part of the 2003 dataset analysed without stereoscopic reconstruction (i.e. mono-mode). The large field of view (FoV $\sim 5^\circ$ diameter) of H.E.S.S. easily encompasses the SN1006 shell, and the angular resolution of $\sim 0.1^\circ$ attained (event-by-event) permits a search for γ -ray sources from different regions associated with the SNR.

2. Analysis & Results

H.E.S.S. observation runs of ~ 28 min duration were taken using the so-called *wobble* mode in which the tracking position is displaced $\pm 0.5^\circ$ in declination with respect to the centre of SN1006 (RA $15^h02^m48.4^s$ Dec $-41^\circ54'42''$ J2000.0). Runs were accepted for analysis if they met a number of quality control criteria based on the recorded CR rate, the number of malfunctioning pixels in each camera and also the tracking performance. In particular telescope tracking was accurate to ~ 20 arcsec for these data and verified by comparing the locations of bright stars in the camera fields of view. Table 1 summarises observations for those runs meeting quality criteria. Without correction for system deadtime the overall observation times were 30h (2003, with $\sim 50\%$ deadtime) and 7h (2004, with $\sim 10\%$ deadtime). A total of 18.2h (2003) and 6.3h (2004) livetime of ON source data (where SN1006 is in the FoV) were available for analysis.

Individual telescope events coincident in time were merged for stereo analysis, followed by Cherenkov image reduction. Image reduction employs image ‘cleaning’ which removes camera pixels dominated by skynoise, flat fielding of the camera responses using a LED flasher, and absolute conversion from pixel ADC counts to photoelec-

Send offprint requests to: Conor.Masterson@mpi-hd.mpg.de & Gavin.Rowell@mpi-hd.mpg.de

* Université Libre de Bruxelles, Faculté des Sciences, Campus de la Plaine, CP230, Boulevard du Triomphe, 1050 Bruxelles, Belgium

** now at Washington Univ., Department of Physics, 1 Brookings Dr., CB 1105, St. Louis, MO 63130, USA

*** now at Department of Physics and Astronomy, Univ. of Sheffield, The Hicks Building, Hounsfield Road, Sheffield S3 7RH, U.K.

tron units using conversion constants obtained from special low-illumination runs. Image moments such as *width* and *length* according to Hillas (1985) are used as a basis to reject the dominating CR background. Rejection of the CR background is achieved by application of image shape cuts (*mean-reduced-scaled-width MRSW* and *mean-reduced-scaled-length MRSL*). A further cut, θ , the difference in assumed and reconstructed event directions is also applied. Event directions are reconstructed according to algorithm ‘1’ as detailed by Hofmann et al. (1999). For a point-like source the combination of cuts on shape, and direction $\theta_{\text{cut}} < 0.14^\circ$ allows for rejection of over 99.9% of CRs whilst retaining $\sim 40\%$ of γ -rays above a threshold energy of 260 GeV (2003) and 110 GeV (2004). The full data processing chain and CR rejection applied to these data were defined *a-priori* using Monte Carlo simulations of γ -ray and real CR events, and fully verified on the Crab Nebula. Details can be found in Aharonian et al. (2004).

The skymap in Fig. 1 presents the excess significance for γ -ray like events (i.e. after cuts) over the RA/Dec plane centred on SN1006. Data from 2003 and 2004 were combined for these analyses. At each bin position, γ -ray-like events are summed within a circle of radius $\theta_{\text{cut}} < 0.14^\circ$ and the CR background is estimated from a ring region of radius 0.5° surrounding the source region. The ring region is chosen to give a solid angle ratio α of 1:7 between the source and background regions respectively. The skymap bins of Fig. 1 are therefore correlated. The cut $\theta_{\text{cut}} < 0.14^\circ$ is appropriate for point-like γ -ray and marginally extended (\sim few arcmin) emission according to the H.E.S.S. point spread function (PSF). No significant excess suggesting γ -ray emission is evident in the skymap. A very similar skymap is obtained when using the alternative *template* model (Rowell 2003) as a CR background estimate. Event statistics and γ -ray flux upper limits at the 99.9% confidence level, summarised in Table 2, have been calculated for a number of *a-priori* chosen locations based on the X-ray morphology as imaged by ASCA and the results of CANGAROO and HEGRA CT1. The upper limits in the table have assumed a differential photon index of $\Gamma=2$, and later (in Fig. 2) we give the upper limit band for a range of assumed indices (2 to 3). The *a-priori* locations, also indicated in Fig. 1 are defined as:

1. **H.E.S.S. Point:** Upper limit on point-like emission ($E > 0.26$ TeV) at the CANGAROO position using $\theta_{\text{cut}} < 0.14^\circ$ (appropriate for the H.E.S.S. PSF). This is also used as an upper limit for the **NE Rim** position.
2. **CANGAROO Point:** Upper limit at the CANGAROO position using a $\theta_{\text{cut}} < 0.25^\circ$ cut appropriate for the CANGAROO 3.8m PSF and selecting events above their energy threshold ($E > 1.7$ TeV).
3. **CANGAROO Point 2003:** As above using only 2003 data.
4. **CANGAROO Point 2004:** As above using only 2004 data.

5. **High Energy Point:** Excess events at the CANGAROO position using $\theta_{\text{cut}} < 0.14^\circ$ cut appropriate to the H.E.S.S. PSF but with an energy threshold $E > 18$ TeV to compare with the HEGRA CT1 result (Vitale et al. 2003). Due to low statistics, the background is estimated from the full FoV (radius 2.0°) excluding the source region and corrected for differences in expected FoV efficiency. The dominant error comes from the on count statistics.
6. **Whole SNR:** Entire SNR at the remnant centre using $\theta_{\text{cut}} < 0.50^\circ$, and H.E.S.S. energy threshold of ($E > 0.26$ TeV).
7. **SW Rim:** As for position 1 but centered on the SE rim.

3. Discussion & Conclusions

Comparing the H.E.S.S. upper limits with the fluxes from CANGAROO-I (1996 and 1997 observations) reveals a discrepancy of a factor ~ 10 (see Fig. 2). It is also clear that no γ -ray emission arises in just one of the years that H.E.S.S. has observed, 2003 nor 2004 (see results given in Table 2 for the CANGAROO position, 2003 and 2004 respectively). Thus H.E.S.S. observations do not confirm the previously-published CANGAROO fluxes for SN1006. One would have to invoke a γ -ray flux variation over timescales less than 1 percent of the SNR age of an order of magnitude, in order to explain the non-detection by H.E.S.S. This is however quite unlikely to occur within the long-accepted diffusive shock acceleration framework for particle acceleration in SNR.

The HEGRA CT1 telescope observed SN1006 at very large zenith angles and obtained a preliminary flux of $F(E > 18 \text{ TeV}) = 2.5 \pm 0.5_{\text{stat}} \times 10^{-13} \text{ ph cm}^{-2} \text{ s}^{-1}$ (Vitale et al. 2003). We applied a matching high threshold cut to H.E.S.S. data and obtained zero counts on source, (with $s - ab = -0.14$ excess events). The 99.9% upper limit on this is a Poisson distribution with a mean of 7 events (we take here the dominant error in the on source counts s and quote the Poisson error). In comparing with the HEGRA CT1 result one must also take into consideration the systematic uncertainty on this flux, estimated to be $\geq 35\%$ (Vitale et al. 2003). Given our exposure and considering both statistical and (uncorrelated) systematic uncertainties, the HEGRA CT1 flux would yield 11 ± 6 excess counts if seen by H.E.S.S. The lower fluctuated value, at 5 counts, is consistent with our observed zero counts with a chance probability of $\sim 7 \times 10^{-3}$. We also include in Fig. 2 the 99.9% upper limit for the whole SNR as a function of energy. This allows comparison in cases where emission from models is predicted from regions not necessarily restricted to the NE and SW rims.

The H.E.S.S. upper limits permit estimation of important parameters for SN1006, in the framework of this source as a particle accelerator. One can firstly estimate an upper limit to the γ -ray luminosity as $L_\gamma = 4\pi F d^2 \text{ erg s}^{-1}$ for a γ -ray flux F and source distance d . Distance estimates for SN1006 are in the range $d \sim 0.7$ to 2.0 kpc,

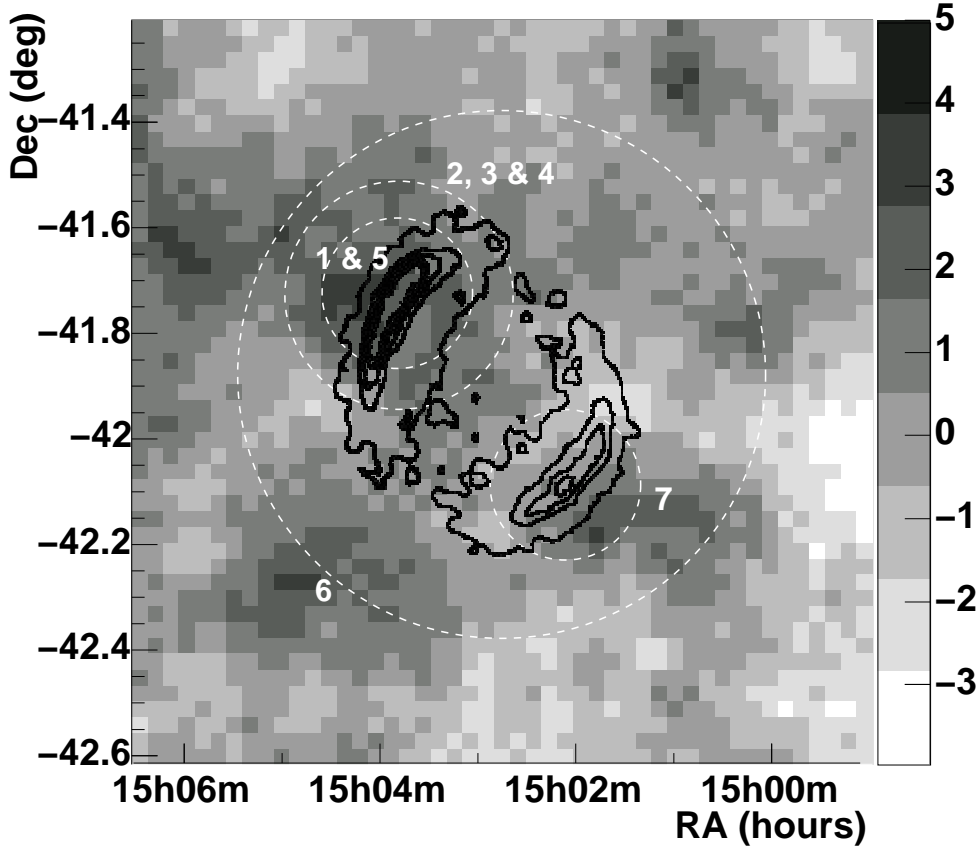


Fig. 1. Skymap of excess significance (according to Eq. 17 of Li & Ma (1983)) centred on SN1006. Indicated are all *a-priori* integration regions used in these analyses (numbered according to the text and Table 2) and ASCA X-ray contours highlighting the X-ray emission from the NE and SW rims. The distribution of significances is fit by a Gaussian distribution with a mean $\mu = -0.016 \pm 0.004$ and sigma $\sigma = 1.035 \pm 0.003$.

(see Allen et al. 2001 for a recent summary of measurements). Taking the H.E.S.S. upper limit for the whole SNR ($E > 0.26$ TeV), distance $d = 2.0$ kpc, assuming a differential photon spectrum of $\Gamma = 2$ and energy range 0.26 to 10 TeV gives $L_\gamma < 1.7 \times 10^{33}$ erg s $^{-1}$. This applies to the present epoch of SNR evolution for SN1006 which is likely in the early Sedov phase (Berezhko et al. 2002). We also estimate the energy in the corresponding accelerated protons W_p over the SNR lifetime as $W_p \sim L_\gamma \tau_{pp}$ erg. The W_p estimate applies to protons of energy $E_p \sim 1.5$ to 60 TeV, and accounts for the average inelasticity (~ 0.17) of converting energy from protons to γ -rays in this scheme. The rather energy independent characteristic lifetime τ_{pp} of accelerated protons interacting with an ambient matter of density n cm $^{-3}$ ($p + p \rightarrow \pi^0 + X \rightarrow 2\gamma + X$) is $\tau_{pp} \sim 4.5 \times 10^{15} (n/\text{cm}^{-3})^{-1}$ sec. With L_γ derived above we arrive at $W_p < 7.8 \times 10^{48} (n/\text{cm}^{-3})^{-1}$ erg. Values for n are in the range $n = 0.05$ to ~ 0.3 cm $^{-3}$ based on X-ray and optical observations. Adopting the lowest value $n = 0.05$ cm $^{-3}$ of the range of densities yields the upper limit $W_p < 1.6 \times 10^{50}$ erg. The choice of n in the W_p estimate should reflect the average density of ambient matter

inside the remnant undergoing interaction with the downstream cosmic-rays (which are assumed to be confined inside the SNR). A lower limit on this value would be that of the ambient matter. We can account for the fact that the energy band of H.E.S.S. observations corresponding to protons (~ 1.5 to 60 TeV) is a fraction ~ 0.25 of the total expected energy in protons over a much wider range of energies covering the cosmic-ray spectrum up to the knee (we assume here ~ 1 GeV to 3 PeV with a differential particle index of -2). Given this, an upper limit on the full proton budget would be $W_p < 6.3 \times 10^{50}$ erg.

Under the synchrotron/IC (scattering on the ubiquitous cosmic microwave background) scenario, knowledge of the synchrotron X-ray flux f_x and TeV IC flux f_γ arising from the *same* electrons permits a clear constraint on the B field in the shock-compressed regions (downstream from the shock) of the SNR according to $f_\gamma(E_\gamma)/f_x(E_x) \sim 0.1(B/10\mu\text{G})^{-2}\xi$ (Aharonian et al. 1997). It is assumed here that the X-ray and γ -ray emitting regions are of the same size, and thus the filling factor $\xi \sim 1$. Such a case arises for high B fields when electrons rapidly cool at their synchrotron production regions. High val-

Table 2. Event statistics and flux upper limits (using the method of Feldman & Cousins 1998, assuming a differential photon index $\Gamma = 2$) for a number of *a-priori*-chosen regions associated with SN 1006: *s* - source events; *b* - CR background estimate; Normalisation factor α ; See text for an explanation of the various regions. Except for limits 3 and 4, numbers are derived exclusively from combined 2003 and 2004 H.E.S.S. data.

Region	^a RA	^a Dec	θ_{cut}	<i>s</i>	<i>b</i>	α	^b S	^c $\phi_{99.9\%}$
1. H.E.S.S. Point ($E > 0.26$ TeV) (also NE rim)	15 ^h 03 ^m 48 ^s	−41°45′	0.14°	1072	6854	0.150	1.19	2.19
2. CANGAROO Point ($E > 1.7$ TeV)	15 ^h 03 ^m 48 ^s	−41°45′	0.25°	127	792	0.153	0.48	0.34
3. CANG. Point ($E > 1.7$ TeV) (2003 H.E.S.S. Data)	15 ^h 03 ^m 48 ^s	−41°45′	0.25°	56	309	0.152	1.2	0.45
4. CANG. Point ($E > 1.7$ TeV) (2004 H.E.S.S. Data)	15 ^h 03 ^m 48 ^s	−41°45′	0.25°	71	483	0.154	−0.35	0.49
5. H.E. Point ($E > 18$ TeV)	15 ^h 03 ^m 48 ^s	−41°45′	0.25°	0	20	0.0069	−	0.18 ^d
6. Whole SNR ($E > 0.26$ TeV)	15 ^h 02 ^m 48.4 ^s	−41°54′42″	0.50°	13358	63113	0.217	−2.8	2.39
7. SW Rim ($E > 0.26$ TeV)	15 ^h 02 ^m 4 ^s	−42°06′3″	0.14°	1042	6754	0.150	0.80	1.98

a. RA & Dec J2000.0 epoch

b. Significance from Eq. 17 of Li & Ma 1983, using normalisation factor α

c. $\phi_{99.9\%}^{ph} = 99.9\%$ integral upper limit ($\times 10^{-12}$ ph cm^{−2}s^{−1})

d. Dominant error is from *s*. We quote here the 99.9% upper limit, which for a Poisson of mean zero is 7 counts.

ues for $B > 40\mu\text{G}$ are in fact implied by X-ray observations and subsequent interpretation in the diffusive shock acceleration framework (Allen et al. 2001, Berezhko et al. 2002, 2003, Bamba et al. 2003, Yamazaki et al. 2004, Ksenofontov et al. 2004). With the H.E.S.S. upper limits on the γ -ray emission, one can therefore estimate a lower limit on the *B*-field. The synchrotron (E_x) and IC (E_γ) photon energies are coupled according to $E_\gamma \sim 1.5(E_x/0.1\text{keV})(B/10\mu\text{G})^{-1}$ TeV, requiring that the fluxes f_x and f_γ in appropriate energy ranges be compared. Comparing the available X-ray energy flux ($E = 0.1$ to 2 keV) $f_x = 1.42 \times 10^{-10}$ erg cm^{−2}s^{−1} (Allen et al. 2001) with that of H.E.S.S. (upper limit energy flux for the whole SNR over an appropriate energy range $E \sim 1$ to 10 TeV and assuming a -2.0 spectral index) at $f_\gamma = 2.29 \times 10^{-12}$ erg cm^{−2}s^{−1} yields a lower limit of $B > 25\mu\text{G}$. This lower limit on *B* is consistent with values discussed earlier which result from comparisons of X-ray observations with detailed theory. In summary, H.E.S.S. observations of SN1006 have not revealed evidence for TeV γ -ray emission. The resulting upper limits will be valuable in constraining further the parameters of γ -ray production in SN1006 (see e.g. Aharonian & Atoyan 1999; Berezhko et al. 2002, Ksenofontov et al. 2004).

Acknowledgements. The support of the Namibian authorities and of the University of Namibia in facilitating the construction and operation of H.E.S.S. is gratefully acknowledged, as is the support by the German Ministry for Education and Research (BMBF), the Max Planck Society, the French Ministry for Research, the CNRS-IN2P3 and the Astroparticle Interdisciplinary Programme of the CNRS, the U.K. Particle Physics and Astronomy Research Council (PPARC), the IPNP of the Charles University, the South African Department of Science and Technology and National Research Foundation, and by the University of Namibia. We appreciate the excellent work of the technical support staff in Berlin, Durham, Hamburg, Heidelberg, Palaiseau, Paris, Saclay, and in Namibia in the construction and operation of the equipment.

References

- Aharonian F.A., Atoyan A.M., Kifune T., 1997, MNRAS 291, 162
 Aharonian F.A., Atoyan A.M. 1999 A&A 351, 330
 Aharonian F.A., Akhperjanian A.J., Aye K.M. et al. 2004 A&A *in prep.*
 Allen G.E., Petre R., Gotthelf E.V. 2001 ApJ 558, 739
 Bamba A., Ueno M., Nakajima H., Koyama K. 2003 ApJ 589, 827
 Berezhko E.G., Ksenofontov L.T., Völk H.J. 2002 A&A 395, 943
 Berezhko E.G., Ksenofontov L.T., Völk H.J. 2003 A&A 412, L11
 Bernlöhr K., et al. 2003 Astropart. Phys. 20, 111
 Cornils R., et al. 2003 Astropart. Phys. 20, 129
 Drury L.O’C, Aharonian F.A., Völk H.J. 1994 A&A 287, 959
 Feldman G.J., Cousins R.D. 1998 Phys. Rev. D57, 3837
 Funk S., Hermann G., Hinton J. et al. 2004 Astropart. Phys. 22, 285
 Hara S., Tanimori T., Kubo H., et al. 2001 In Proc. 27th ICRC Hamburg 5, 2455
 Hillas A. 1985 In Proc. 19th ICRC (La Jolla) vol 3, 445
 Hofmann W., Jung I., Konopelko A. et al. 1999 Astropart. Phys. 10, 275
 Koyama K., Petre R., Gotthelf E.V. et al. 1995 Nature, 378
 Ksenofontov L.T., Berezhko E.G., Völk H.J. 2004 in Proc. Symp. on High Energy Gamma-Ray Astronomy (Heidelberg), AIP Press *in press*
 Li T.P., Ma Y.Q. 1983 ApJ 272, 317
 Long K.S., Reynolds S.P., Raymond J.C. et al. 2003 ApJ 586, 1162
 Naito T., Takahara F. 1994 J. Phys. G: Nucl. Part. Phys. 20, 477
 Naito T., et al. 1999 Astron. Nachr. 320, 205
 Masterson C. et al. 2003 Proc. 28th ICRC Tsukuba OG2.2, 2323
 Rowell G.P. 2003 A&A 410, 389
 Tanimori T., Hayami Y., Kamei S., et al. 1998 ApJ, L25
 Tanimori T., Naito T., T. Yoshida T., et al. 2001 In Proc. 27th ICRC Hamburg, vol 5, 2465

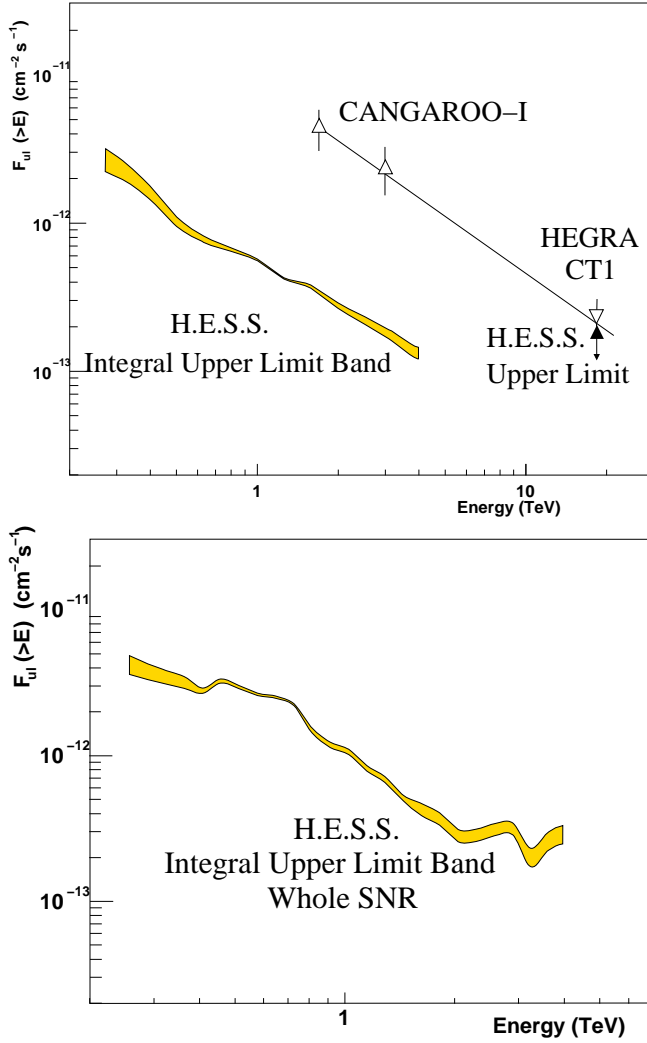


Fig. 2. Top: Comparison of experimental results for SN1006 from H.E.S.S. (integral upper limit 99.9% c.l. band at the CANGAROO position using $\theta_{\text{cut}} < 0.23^\circ$, see Table 2), CANGAROO-I fluxes of Tanimori et al. (1998) and the HEGRA CT1 flux of Vitale et al. (2003). The solid line joins the two CANGAROO-I fluxes and is extended up to the HEGRA CT1 flux. The high energy H.E.S.S. upper limit is shown for comparison with the HEGRA CT1 flux. The H.E.S.S. UL band arises when assuming a differential spectral index from $\Gamma=2$ to 3. **Bottom:** H.E.S.S. upper limit band for the whole SNR, after cuts described in the text. The band arises when assuming a differential spectral index of $\Gamma=2$ to 3.

Vincent P., et al. 2003 Proc. 28th ICRC, Tsukuba, Univ. Academy Press Tokyo, 2887

Vitale V., et al. 2003 In Proc. 28th ICRC Tsukuba, OG2.2, 2389

Yamazaki R., Yoshida T., Terasawa T., et al. 2004 A&A 416, 595